# Perfusion functional MRI reveals cerebral blood flow pattern under psychological stress

Jiongjiong Wang*†‡, Hengyi Rao§, Gabriel S. Wetmore†§, Patricia M. Furlan¶, Marc Korczykowski†§, David F. Dinges¶‖, and John A. Detre*†‡§

Departments of *Radiology, §Neurology, ¶Psychiatry, and ‖Psychology and †Center for Functional Neuroimaging, University of Pennsylvania, Philadelphia, PA 19104

Despite the prevalence of stress in everyday life and its impact on happiness, health, and cognition, little is known about the neural substrate of the experience of everyday stress in humans. We use a quantitative and noninvasive neuroimaging technique, arterial spin-labeling perfusion MRI, to measure cerebral blood flow (CBF) changes associated with mild to moderate stress induced by a mental arithmetic task with performance monitoring. Elicitation of stress was verified by self-report of stress and emotional state and measures of heart rate and salivary-cortisol level. The change in CBF induced by the stress task was positively correlated with subjective stress rating in the ventral right prefrontal cortex (RPFC) and left insula/putamen area. The ventral RPFC along with right insula/putamen and anterior cingulate showed sustained activation after task completion in subjects reporting a high stress level during arithmetic tasks. Additionally, variations of baseline CBF in the ventral RPFC and right orbitofrontal cortex were found to correlate with changes in salivary-cortisol level and heart rate caused by undergoing stress tasks. We further demonstrated that the observed right prefrontal activation could not be attributed to increased cognitive demand accompanying stress tasks and extended beyond neural pathways associated with negative emotions. Our results provide neuroimaging evidence that psychological stress induces negative emotion and vigilance and that the ventral RPFC plays a key role in the central stress response.

anterior cingulate cortex | arterial spin labeling | right prefrontal cortex

Stress is common in everyday life and is believed to affect happiness, health, and cognition (1–7). Although considerable progress has been made in uncovering the neuroendocrine and molecular processes mediating the cascade of reactions to stressors (8, 9), the central mechanism and neural correlates of psychological stress remain unknown. Manifestations of the fight-or-flight response under life-threatening situations suggest that the brain's response to stress may (at least) involve excitation of the emotion and vigilance systems and inhibition of appetitive goals. For instance, a prey evading a predator is in constant fear and high alert, with suppressed function for food intake and reproduction (5). Although the majority of stress today is due to psychosocial factors and is not life-threatening, this stereotyped brain-activation pattern may still take place during a test or job interview and has been modeled by using the performance of an impromptu speech (10). This hypothesis is supported by neurochemical studies indicating that a common denominator of the response to stress in the brain, secretion of corticotrophin-releasing hormone and norepinephrine, causes symptoms including arousal, fear-related behavior, and suppressed appetite (8, 9).

Recent neuroimaging studies have greatly enriched understanding of the neuroanatomical substrates underlying perception, cognition, and emotion. Data on emotional processes suggest a common neural network involving the prefrontal cortex, amygdala, insula, basal ganglia, and anterior cingulate (11, 12). In particular, negative affect generally elicits activation in the right prefrontal cortex (RPFC), amygdala, and insula, whereas the left prefrontal cortex is associated with positive emotion and appetitive goals along with reward-related cortical regions (13). The neural correlates of vigilance and sustained attention have been largely localized to the right prefrontal and parietal lobe and the thalamus (14). The right prefrontal cortex may play a key role in the brain's response to stress, because this brain area is a primary part of both the emotion and vigilance networks. Neurons that are either the target or the releasing site of an array of stress mediators (neurotransmitter and hormone) have been identified in that area (8, 9). High levels of right-sided prefrontal activation have been linked with negative affective style and suppressed immune function (15, 16), suggesting that this brain area may be a common mediator of the relationship between psychosocial stress and its effects on mental and physical health (1–3, 6, 7).

To date, there is little direct neuroimaging evidence concerning the central mechanism of the "normal" stress response. Although dysfunction of amygdale, prefrontal cortex, and hippocampus has been suggested in posttraumatic stress disorder (17), the validity of generalizing these findings to the normal cerebral processing underlying everyday psychological stress is uncertain. This work aims to fill in this gap by employing a quantitative functional MRI (fMRI) technique, arterial spin-labeling perfusion MRI (18), to study the central circuitry of psychological stress. This technique directly measures cerebral blood flow (CBF) by using arterial blood water as an endogenous contrast agent. With excellent reproducibility over long-term time periods (19, 20) and minimal sensitivity to magnetic-field inhomogeneity effects (21), perfusion fMRI is ideal for imaging a sustained behavioral state, such as stress, that involves the function of deep brain structures. Perfusion fMRI also allows ecological paradigms to be used in the MR scanner to induce "natural" stress, owing to its reduced scanner noise level and reduced sensitivity to subject motion (22).

## Methods

**Subjects.** Thirty-two subjects participated in this study. Twenty-five subjects (age 24.1 ± 2.8 yrs, 12 female) participated in the stress experiment and 7 subjects (age 23.4 ± 1.3 yrs, 4 female) participated in the control experiment. Two of the 25 subjects participating in the stress experiment were excluded because of incomplete behavioral data and abnormally high baseline salivary cortisol level (>3 SD), resulting in 23 complete data sets (11 female) for stress tasks. All of the subjects were native English speakers and screened for history of neurologic and psychiatric disease. Written informed consent was obtained before all

human studies, in accord with an Institutional Review Board approval from the University of Pennsylvania.

**Experimental Procedures.** We adapted the mental arithmetic task as the psychological stressor during perfusion fMRI scans (23, 24). Subjects were instructed to perform serial subtraction of 13 from a four-digit number and respond verbally. During the task, the subjects were prompted for faster performance and were required to restart the task if an error occurred. This high-stress condition was preceded by a low-stress condition, during which subjects counted aloud backward from 1,000 (to control for activation of verbal and auditory centers). Subjects were given a 15-min resting period after they arrived at the MR facility. The scanning protocol consisted of four perfusion fMRI scans (8 min each) and an anatomical scan (6 min) at the end. During the second and third perfusion fMRI scans, subjects were instructed (at the beginning of each session) to perform the counting-backward (low-stress) and serial-subtraction (high-stress) task. The low- and high-stress scans were conducted in a fixed order to eliminate contamination of the control condition by increased emotional reactivity elicited by the high-stress task. The first and last perfusion fMRI scans were baseline conditions without task.

Self-report of stress and anxiety level (on a scale of 1 to 9) and saliva samples (using a cotton swab placed in the mouth for 2 min) were collected right after the subjects entered the MR scanner and after each MR scan. Subjects were also required to report the level (on a scale of 1 to 9) of effort, frustration, and task difficulty after the low- and high-stress tasks. Throughout the experiment, heart rate was recorded every 2 min, based on a pulse-oxymetry reading. Saliva samples were stored at −80°C until assayed. To measure stress caused by undergoing MR scanning, we conducted a control experiment using the same scanning protocol, but the subjects were not required to perform any task. Self-report of stress, heart-rate recording, and saliva-sample collection were as described in the stress experiment. All MRI experiments were carried out between 3 p.m. and 5 p.m. to control for diurnal fluctuations in salivary-cortisol level.

**Imaging-Data Acquisition.** MR scanning was conducted on a 3.0T Trio whole-body scanner (Siemens, Erlangen, Germany), using a standard transmit/receive head coil. A continuous arterial spin-labeling (CASL) technique (25) was used for perfusion fMRI scans. Interleaved images with and without labeling were acquired by using a gradient-echo echo-planar imaging sequence. A delay of 1 sec was inserted between the end of the labeling pulse and image acquisition to reduce transit artifact. Acquisition parameters were field of view (FOV) = 22 cm, matrix = $64 \times 64$, repetition time (TR) = 4 sec, echo time (TE) = 17 ms, and flip angle = 90°. Fourteen slices (6 mm thick with 1.5-mm gap) were acquired from inferior to superior in a sequential order. Each CASL scan with 120 acquisitions took 8 min. A 3D magnetization-prepared rapid gradient echo volumetric scan was used for high resolution T1-weighted anatomic images: TR = 1,620 ms, inversion time (TI) = 950 ms, TE = 3 ms, flip angle = 15°, 160 contiguous slices of 1.0-mm thickness, FOV = $192 \times 256$ mm$^2$, matrix = $192 \times 256$, 1NEX with a total scan time of 6 min.

**Behavioral and Physiological Data Analysis.** The salivary-cortisol level was assayed by using an enzyme immunoassay kit (Salimetrics, State College, PA). Behavioral and physiological measurements were analyzed by using repeated-measures ANOVA of the program SPSS 12.0 (SPSS, Chicago) to assess the effect of experimental condition. The differences of the behavioral and physiological measures between the low- and high-stress tasks were entered into a cross-correlation analysis to search for any significant correlation between these measurements across subjects. Because salivary cortisol is a delayed peripheral response (23), the immediate measurements after stress tasks may not reflect variations in
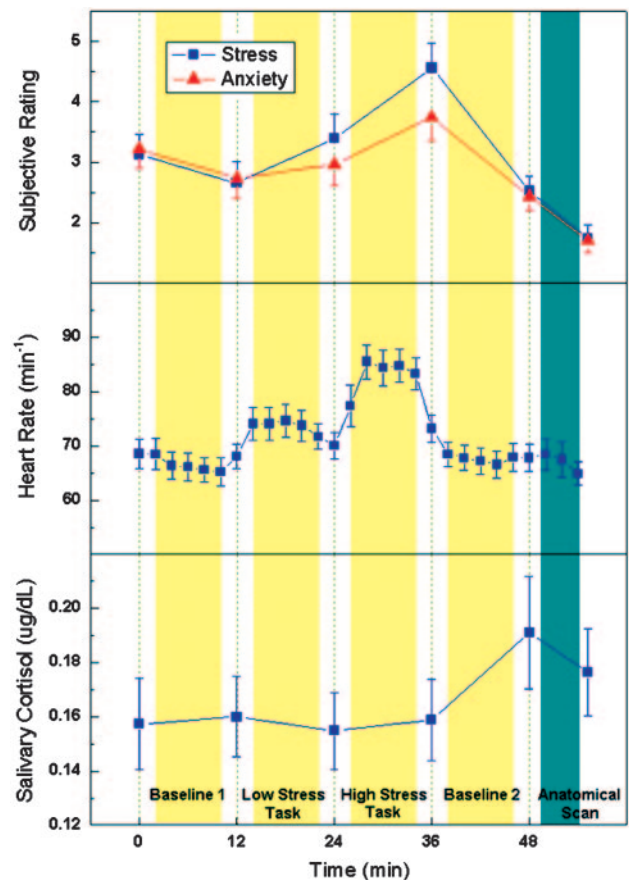


**Fig. 1.** Average subjective ratings of stress and anxiety, heart rate, and salivary-cortisol level during the time course of the stress experiment. Time 0 indicates the start of MRI experiments. The yellow columns represent the perfusion fMRI scans (each 8 min) and the dark green column represents the anatomical scan. Behavioral ratings and salivary-cortisol samples were taken between scans, whereas heart rate was continuously recorded every 2 min. Note that the peak in salivary-cortisol level lags behind other measures. The error bars indicate standard error.

subjects' stress state. Therefore, we measured the area under the curve (AUC) of the salivary cortisol level, calculated as the net area under the stress-response curve (all six samples, see Fig. 1), with reference to the baseline (first sample) by using trapezoidal integration (26).

**Imaging-Data Analysis.** Perfusion fMRI data were analyzed offline by using the program VOXBO (www.voxbo.org) and SPM99 software packages (Wellcome Department of Cognitive Neurology, Institute of Neurology, London). MR image series were first realigned to correct for head movements, coregistered with each subject's anatomical MRI, and smoothed in space with a 3D, 12-mm full-width at half-maximum Gaussian kernel. Perfusion-weighted image series were generated by pairwise subtraction of the label and control images, followed by conversion to absolute CBF image series based on a single compartment continuous arterial spin-labeling perfusion model (25). Voxel-wise analyses of the CBF data were conducted in each subject by using a general linear model (GLM), including the global time course as a covariate to reduce the effect of spatially coherent noise (27) (first-level analysis). No temporal filtering or smoothing was involved. Two contrasts were defined in the GLM analysis, namely the CBF difference between the two stress tasks (high-stress and low-stress) and the CBF difference between the two baseline conditions (baseline 2 − baseline 1).

NEUROSCIENCE

**Table 1. Self-report of effort, difficulty, and frustration during the low- and high-stress tasks (scale 1–9)**

| Stress | Effort | Difficulty | Frustration |
|---|---|---|---|
| Low-stress task | 4.4 (0.5) | 3.4 (0.4) | 3.4 (0.4) |
| High-stress task | 7.0 (0.3) | 6.6 (0.3) | 6.1 (0.4) |

Data are presented as mean (standard error).

Individual contrast images ($\beta$ maps for each contrast) were normalized into a canonical space (Montreal Neurological Institute standard brain), and were analyzed by using one-sample $t$ tests to obtain the activation pattern for the two defined contrasts using a random-effects model that allows population inference (second-level analysis). This step provides a within-subject comparison of CBF between corresponding experimental conditions. Furthermore, linear-regression analyses were carried out on these normalized individual maps to obtain the activation pattern correlated with perceived stress and other measurements, by using differences in each of the behavioral and physiological measurements between the high- and low-stress tasks as the independent variable. For salivary cortisol, we used the AUC measurement as the independent variable for regression analyses. Areas of significant activation were identified at the cluster level for the $P$ value $<0.005$ (uncorrected) and the cluster extent size $>94$ voxels ($2 \times 2 \times 2$ mm$^3$), resulting in a cluster-corrected threshold of $P < 0.05$ in SPM99. Regions of interest (ROIs) based on activation clusters were generated by using the SPM MARSBAR toolbox. To test the asymmetry of prefrontal activation, the right prefrontal ROI was also flipped in the left–right direction to generate the left homologous ROI. CBF changes of the 23 subjects in these ROIs were extracted and entered into a univariate GLM analysis using the SPSS software to investigate the effect size of each covariate.

## Results

**Behavioral and Physiological Data.** The results of subjects' self-ratings of stress, emotion, and physiological responses suggest that the stress-elicitation paradigm successfully induced a mild-to-moderate level of psychological stress. Average self-report of stress ($P = 0.002$) and anxiety ($P = 0.008$) levels and the heart rate ($P < 0.001$) increased from the low-stress task to the high-stress task and decreased during the second baseline period (Fig. 1). Salivary cortisol, a stress-related hormone, reached its peak 10 min after the end of the high-stress task ($P = 0.045$), consistent with the expected time lag between peripheral cortisol and behavioral measures (23). Subjects' ratings of task difficulty ($P < 0.001$), effort required ($P < 0.001$), and frustration ($P < 0.001$) were significantly elevated in the high-stress condition relative to the low-stress condition (see Table 1). In addition, we found that perceived stress level was significantly correlated with perceived anxiety level across subjects ($r = 0.74$, $P < 0.001$) and was, to a lesser extent, correlated with perceived frustration ($r = 0.39$, $P = 0.064$). The correlation between self-ratings of task difficulty and effort required also showed a trend toward significance ($r = 0.40$, $P = 0.057$). During the control experiment, none of the behavioral and physiological measures showed significant variation ($P > 0.12$) (see Fig. 5, which is published as supporting information on the PNAS web site), suggesting that undergoing MRI scanning caused little effect on subjects' stress and emotional state.

**Imaging Data, Regression Analysis with Perceived Stress.** Regression analyses were carried out to search for the specific brain regions associated with individual subject's experience of stress. The hypothesis was that the CBF change induced by the high-stress task compared with the low-stress task should be correlated with the change in perceived stress between these two conditions. We found a positive correlation between the changes in CBF and subjective
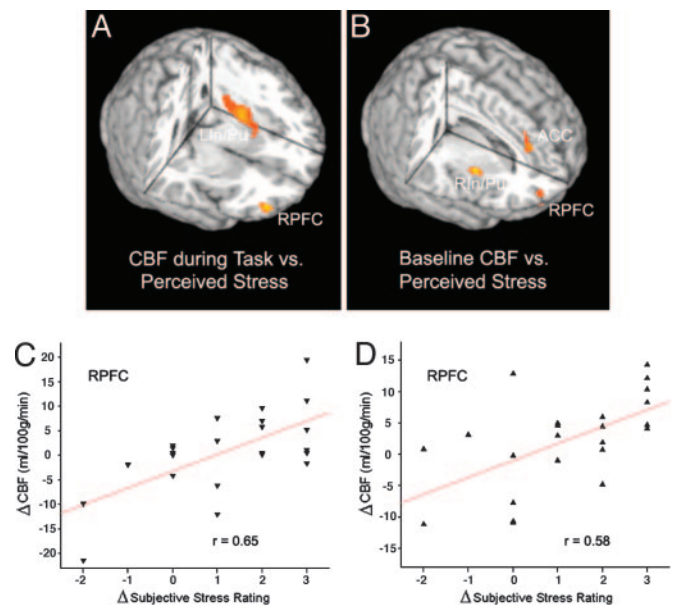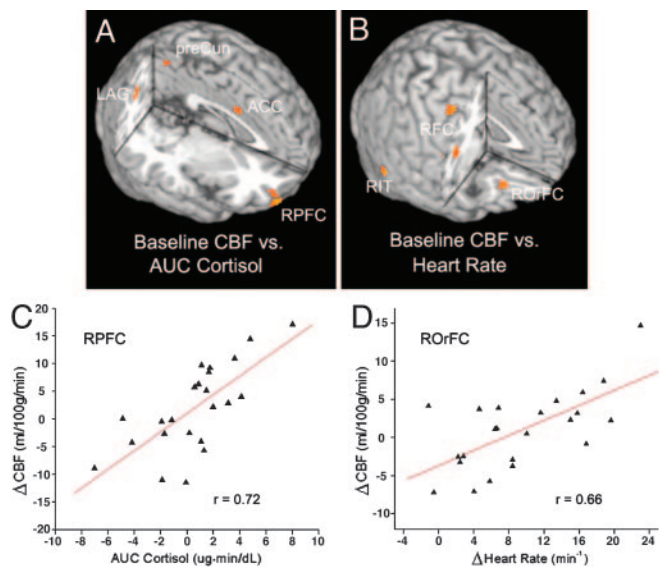


**Fig. 2.** Three-dimensional rendering of the regression-analysis results, which use the CBF change during stress tasks (high-stress − low-stress task) (A) or the CBF change at baseline (baseline 2 − baseline 1) (B) as the dependent variable and the change in perceived stress from the low- to high-stress task as the predictor. Also shown are scatterplots of changes in CBF during stress tasks (C) and at baseline (D) as a function of changes in perceived stress between the two stress tasks. Each data point represents one subject. Mean CBF values are drawn from the ROI defined by the activation cluster. RPFC $x = 42$, $y = 54$, $z = -10$, 211 pixels, $Z = 3.59$ in A; $x = 32$, $y = 58$, $z = -2$, 118 pixels, $Z = 2.98$ in B. ACC $x = 10$, $y = 38$, $z = 24$, 156 pixels, $Z = 3.22$; LIn/Pu $x = -32$, $y = -8$, $z = 4$, 811 pixels, $Z = 3.46$; right insula/putamen (RIn/Pu) $x = 38$, $y = 2$, $z = 2$, 144 pixels, $Z = 3.73$.

stress rating in the ventral RPFC (Fig. 2A). A significant correlation was also observed in the left insula/putamen (LIn/Pu) area. The scatterplot of Fig. 2C shows that the serial-subtraction task yielded a greater CBF increment in the ventral RPFC in subjects who reported larger amount of stress elevation.

We conducted a regression analysis to determine whether there was any lasting effect of psychological stress on resting state CBF, even after the stressor disappeared. The hypothesis was that the CBF difference between the two baseline conditions (baseline 2 − baseline 1) should be correlated with the change in self-report of stress from the low- to high-stress task. Again, we detected a significant correlation between changes in baseline CBF and subjective stress rating during tasks in the ventral RPFC (Fig. 2B). Positive correlations were also observed in the anterior cingulate cortex (ACC) and right insula/putamen. As displayed in the scatterplot of Fig. 2D, greater baseline CBF increment in the ventral RPFC was associated with larger increases in perceived stress during tasks.

**Imaging Data, Regression Analysis with Physiological Stress Responses.** We went on to test whether the observed RPFC activation can be replicated when measures of physiological stress responses were used as the predictor in regression analyses. Indeed, we found that changes in baseline CBF pre- and poststress tasks (baseline 2 − baseline 1) were significantly correlated with the cumulative salivary cortisol change (AUC measures) in the ventral RPFC (Fig. 3A). Fig. 3A also indicates several other brain regions manifesting significant association between changes in baseline CBF and AUC measures of cortisol, including ACC, and precuneus and left and right angular gyri/inferior parietal cortex. When heart rate was used as the covariate in regression analyses, we found significant associations between variations in baseline CBF (baseline 2 −

**Fig. 3.** Three-dimensional rendering of the regression-analysis results, which use the CBF change at baseline (baseline 2 − baseline 1) as the dependent variable and the AUC measures of salivary-cortisol level (*A*) or the change in heart rate from the low- to high-stress task (*B*) as the predictor. Also shown are scatterplots of mean baseline CBF changes as a function of cortisol (*C*) and heart rate (*D*) in activation clusters. RPFC $x = 30$, $y = 56$, $z = -16$, 406 pixels, $Z = 3.79$; right obitofrontal cortex (ROrFC) $x = 26$, $y = 34$, $z = -16$, 100 pixels, $Z = 3.51$; precuneus (preCun) $x = 6$, $y = -56$, $z = 54$, 205 pixels, $Z = 3.03$; left angular gyrus (LAG) $x = -40$, $y = -64$, $z = 32$, 304 pixels, $Z = 3.15$; right angular gyrus (RAG) $x = 26$, $y = -60$, $z = 40$, 241 pixels, $Z = 3.38$; right frontal cortex (RFC) $x = 56$, $y = -2$, $z = 24$, 233 pixels, $Z = 3.12$ and $x = 32$, $y = -10$, $z = 54$, 198 pixels, $Z = 3.23$; right inferior temporal cortex (RIT) $x = 62$, $y = -54$, $z = -16$, 176 pixels, $Z = 3.68$.

baseline 1) and changes in heart rate from the low- to high-stress task in the right obitofrontal cortex (ROrFC), dorsolateral right frontal cortex, and right inferior temporal cortex. The scatterplots in Fig. 3 *C* and *D* show that undergoing the two stress tasks yielded a greater increment of baseline CBF in the ventral RPFC and ROrFC in subjects manifesting a larger amount of cumulative salivary-cortisol elevation and greater heart-rate increase from the low- to high-stress task, respectively. However, when regression analyses were performed with CBF differences between the low- and high-stress tasks as the dependent variable, we did not observe a significant relationship between RPFC CBF and physiological stress responses. Instead, we found a significant correlation between CBF changes during stress tasks and AUC measures of cortisol in the anteromedial prefrontal cortex (see Fig. 6, which is published as supporting information on the PNAS web site).

To further test the specificity (asymmetry) of the observed ventral RPFC activation with perceived stress and salivary-cortisol level, regression analyses were repeated by using CBF values derived from a left homologous ROI as a covariate along with subjective stress rating or AUC measures of salivary cortisol. The observed RPFC activation was still significant with left prefrontal
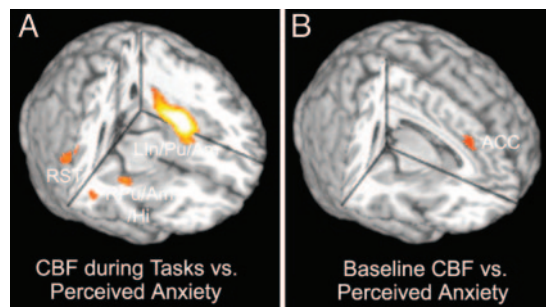
**Fig. 4.** Three-dimensional rendering of the regression-analysis results, which use the CBF change during stress tasks (high-stress − low-stress task) (*A*) or the CBF change at baseline (baseline 2 − baseline 1) (*B*) as the dependent variable and the change in perceived anxiety from the low- to high-stress task as the predictor. LIn/Pu/amygdala (LIn/Pu/Am) $x = -36$, $y = -6$, $z = -4$, 2,379 pixels, $Z = 5.30$; right putamen/amygdala/hippocampus (RPu/Am/Hi) $x = 34$, $y = -12$, $z = -10$, 339 pixels, $Z = 3.21$; right superior temporal cortex (RST) $x = 52$, $y = -44$, $z = 16$, 432 pixels, $Z = 3.58$; ACC $x = 6$, $y = 32$, $z = 32$, 162 pixels, $Z = 2.83$.

CBF included in the regression model. On average, CBF within the left homologous ROI accounted for 17% of the total variance of RPFC CBF, whereas the fractional variance explained by perceived stress and cortisol was 36% and 45%, respectively ($P < 0.02$, Table 2). Furthermore, when the left hemispheric CBF was subtracted from the right hemisphere and used as the dependent variable in the regression analysis, we still observed significant association of ventral RPFC CBF with perceived stress and salivary cortisol (see Fig. 7, which is published as supporting information on the PNAS web site). These data strongly support the specific association of CBF increase in the ventral RPFC and psychological stress.

**Imaging Data, Regression Analysis with Anxiety and Other Behavioral Measures.** Regression analyses were also repeated with subjective anxiety rating as the independent variable. A strong correlation between the changes in CBF and subjective anxiety rating during stress tasks (high-stress task − low-stress task) was observed in a large activation cluster covering left insula/putamen/amygdala (LIn/Pu/Am) and superior temporal regions. Positive correlations between changes in CBF and perceived anxiety level during stress tasks were also evident in right putamen, amygdale, hippocampus, and right superior temporal regions (Fig. 4*A*). A positive correlation between changes in baseline CBF (baseline 2 − baseline 1) and subjective anxiety rating during stress tasks was observed in ACC (Fig. 4*B*). The brain activations associated with perceived anxiety partially overlap those related to perceived stress, consistent with our behavioral data showing a correlation between these two variables. However, RPFC CBF, either during stress tasks or at baseline, was not found to vary with changes in subjective anxiety rating. Further regression analyses indicated that baseline CBF change in the ventral RPFC was correlated with perceived stress, even with perceived anxiety included as a covariate in the regression model (see Fig. 8, which is published as supporting information on the PNAS web site). Table 2 shows that perceived anxiety, when

**Table 2. Univariate analysis of variance of baseline CBF changes in ventral RPFC explained by different covariates and CBF in left homologous ROI**

| Stress | Anxiety | Frustration | Effort | Difficulty | Cortisol | Heart Rate | LPFC CBF | Model |
|---|---|---|---|---|---|---|---|---|
| 0.363 | 0.028 | 0.011 | 0.058 | 0.073 | 0.453 | 0.032 | 0.171 | 0.753 |
| $P = 0.014$ | | | | | $P = 0.004$ | | $P = 0.112$ | $P = 0.003$ |

Results are based on values of partial *R* squared in SPSS, and the model includes all covariates and an intercept. LPFC, left prefrontal cortex.

included with perceived stress and other covariates in the GLM, accounted for little variation in ventral RPFC CBF (<3%). In contrast, significant associations between CBF and anxiety ratings during stress tasks could be observed in LIn/Pu/amygdala and right superior temporal regions when perceived stress was included as a covariate in the regression model. Although behaviorally correlated, perceived stress and anxiety seem to be associated with distinguishable brain-activation patterns which overlap in LIn/Pu and ACC.

We also carried out regression analyses using the self-report of frustration, effort, and difficulty as the independent variables. None of these analyses showed significant activations in the RPFC or ACC (detailed activations are listed in Tables 3–5, which are published as supporting information on the PNAS web site). Inclusion of self-report of frustration, effort, and difficulty along with the stress rating in the regression model did not change the observed activation pattern obtained with stress rating as the single predictor. Further GLM analyses indicate that frustration, effort, and difficulty each accounted for only a small fraction (<10%) of the variance in ventral RPFC CBF (Table 2).

**Imaging Data, Within-Subject Comparison of CBF.** Within-subject comparison of CBF between the high- and low-stress tasks was carried out by using a random-effects model (see Fig. 9, which is published as supporting information on the PNAS web site). Increased CBF was observed in the right insula/putamen, dorsomedial prefrontal cortex/ACC, precuneus/superior parietal gyrus, and left inferior temporal region. Suppressed CBF was observed in the ventrolateral left prefrontal cortex (LPFC) and orbitofrontal cortex (70% on the left side). In addition, there were bilateral deactivation clusters with reduced CBF during the high-stress task relative to the control condition, including pre- and postcentral gyri, insula, superior and middle temporal cortex, and right angular gyrus/inferior parietal cortex. The within-subject comparison of baseline CBF pre- and poststress tasks (baseline 2 − baseline 1) revealed activation in the anterior RPFC, ventrolateral LPFC, thalamus, posterior cingulate cortex, and left inferior temporal cortex, whereas reduced CBF was observed only in the left superior temporal region (see Fig. 10, which is published as supporting information on the PNAS web site).

### Discussion

The major finding from our study is that ventral RPFC activation is specifically associated with psychological stress, and this activity persists even beyond the stress-task period. This mapping between behavioral/physiologic state and neuroanatomy is supported by the association of RPFC CBF changes with both subjective and objective measures of stress responses. Increased cognitive demand and effort accompanying the task stressors cannot explain the present finding, because our regression analyses demonstrated that difficulty or effort did not contribute to RPFC brain activation. Lasting effects of right prefrontal activation were also observed during baseline conditions without any cognitive task, excluding potential confounding effects due to cognitive differences between the two stress tasks.

Earlier neuroimaging and neurophysiological studies suggested that activation in RPFC is associated with negative emotions, especially sadness and fear (28, 29), accompanied by increased vigilance to threat-related cues, as often occurs with certain types of anxiety disorders (13). The ventral RPFC activation observed in our study, therefore, suggests that psychological stress induces negative emotion and vigilance. We also observed activation of LIn/Pu during stress tasks, which has been linked with the processing of certain forms of negative affect, especially disgust (30, 31). The persistence of the ventral RPFC activation, even after completion of stress tasks, may reflect a prolonged state of heightened vigilance and emotional arousal elicited by stressors. Both the ACC, an important region involved in the attentional processing of

emotion (11, 32), and the right insula/putamen showed sustained activation after stress tasks. However, the ventral RPFC activation and, in particular, its lasting effect, was uniquely associated with psychological stress and could not be attributed to emotional responses, including anxiety and frustration, in our study. The detected brain regions associated with anxiety (e.g., insula, putamen, amygdala, and ACC) were highly consistent with existing understanding of emotional networks, supporting the sensitivity and validity of perfusion fMRI. The lasting effect of stress also suggests that perfusion fMRI may be a more suitable approach than the blood-oxygen-level-dependent (BOLD) contrast to study the neural substrates of psychological stress, because subjects could no longer return to a "baseline" state after stress tasks, as assumed in a conventional block design in BOLD fMRI.

The parallel changes between baseline CBF in the ventral RPFC and AUC measures of salivary cortisol is consistent with animal studies showing rich cortisol receptors in prefrontal cortex and in hippocampus and amygdale (8, 9). Additionally, CBF changes during stress tasks were found to be associated with cortisol in the anteromedial prefrontal cortex. The observed correlations between baseline CBF and salivary cortisol in ACC, precuneus, and parietal cortex also concur with earlier studies using nuclear-medicine methods to measure CBF in stress-related disorders (33–35). Cortisol has been shown to contribute to increased arousal, vigilance, and memory formation, along with inhibition of the growth and reproductive systems and containment of the immune response (8, 9). Our data suggest a mechanism whereby peripheral stress hormone may reciprocally affect the central stress response through enhanced neural activity in the ventral RPFC, along with ACC and other brain regions. This speculation is supported by the association of heart-rate increase and right obitofrontal cortex CBF elevation, although excitation of the sympathetic nervous system may not be specific to psychological stress.

The joint correlations of baseline CBF changes in the ventral RPFC with perceived stress, cortisol, and heart rate suggest that sustained regional brain activation after stressors may be a characteristic feature of stress. The time scale of the acute stress response, including its lasting effect, is an important issue in the neurobiology of stress. After a moderately acute stressor, it may take minutes for heart rate and 1–2 h for cortisol to return to the baseline, although behavioral ratings may recover faster (23, 36). We used a mild-to-moderate stressor, which caused elevation in peripheral cortisol that peaked about 10 min after the high-stress task. Given the observed temporal coincidence of RPFC CBF increase and stress-hormone elevation, cortisol might be a mediator of the lasting effect of central stress response. However, this hypothesis needs to be tested further by using cortisol-receptor blockers or giving exogenous cortisol to the subjects.

Concomitant with activation of the ventral RPFC in subjects experiencing stress, we observed CBF reductions in ventrolateral left prefrontal cortex and left orbitofrontal cortex (see Fig. 9) in within-subject comparison of CBF between the high- and low-stress conditions. These latter areas, in conjunction with ventral striatum, subserve the positive-emotion network and reward system that mediates approach-related, appetitive goals (37). Hypoactivation in these circuits has been linked to depression (13). Although perfusion reductions in this positive-reward system were not significantly correlated with measures of stress responses in individual subjects, these results nevertheless suggest an inhibition of brain regions supporting appetitive and hedonic goals during psychological stress. Our within-subject analysis also showed activation of brain areas associated with negative emotions, including right insula and putamen (11, 38), during the high-stress relative to the low-stress task. The observed activation in the dorsomedial prefrontal cortex/ACC and precuneus/parietal cortex may reflect mental arithmetical performance (39) and assessment of the mental state (40) during the serial-subtraction task, whereas the CBF reduction in pre- and postcentral gyri and temporal cortex may reflect more frequent

verbal movement and greater auditory stimulation during counting backward versus serial subtraction. The within-subject comparison of CBF pre- and poststress tasks yielded a mixed picture of the lasting effect of stress. Whereas activations in the thalamus and posterior cingulate cortex have been reported in neuroimaging studies on emotional distress (38, 41), the ventrolateral left prefrontal cortex activation and suppressed activity in the left superior temporal cortex may suggest a more relaxed state in the group of subjects relative to the first baseline, in line with the mean behavioral responses shown in Fig. 1. Nevertheless, anterior RPFC activation can still be detected at the group level, lending further support to our regression-analysis results.

The experimental paradigm used required subjects' active efforts to meet a challenge (42), which mimics the common experience of keeping up with the pace of life. The task induced mild-to-moderate levels of psychological stress (23), well within the range of everyday stress. Care has to be taken in generalizing the observed pattern of neural activation to chronic and severe stress, because neural activation may vary with stress level following an inverted U-shape function (43). Animal studies have shown that chronic stress causes remodeling of neurons in the medial prefrontal cortex, amygdala, and hippocampus (44–46). In humans, atrophy of the ventromedial prefrontal cortex has been reported in major recurrent depression (47). The observed suppression of neural activity in the positive-reward system, if prolonged because of chronic stress, might lead to changes in the brain that could impair cognitive function and affect systemic processes (6, 7). Moreover, sustained activation of the ventral RPFC is likely to contribute to the adverse effects of chronic stress on physical health and personality (48), because right-sided prefrontal activation has been linked with suppressed immune function and negative affective style (15, 16). Although the brain's response to acute stress may be protective, a chronically stressed brain may be incrementally and deleteriously remodeled through the repeated neural activation pattern and sustained hyperactivity of the hypothalamus–pituitary–adrenal axis (44–46).

In summary, regional brain activity associated with both behavioral and physiological stress responses has been probed by using perfusion fMRI. The localization of brain regions related to emotion, vigilance, and goal-directed behavior within the RPFC suggests that this region serves a central role in coordinating a range of biological and behavioral responses to stress (49).

1. Segerstrom, S. C. & Miller, G. E. (2004) *Psychol. Bull.* **130**, 601–630.
2. Cohen, S., Tyrrell, D. A. J. & Smith, A. P. (1993) *J. Personality Social Psychol.* **64**, 131–140.
3. Caspi, A., Sugden, K., Moffitt, T. E., Taylor, A., Craig, I. W., Harrington, H., McClay, J., Mill, J., Martin, J., Braithwaite, A. & Poulton, R. (2003) *Science* **301**, 386–389.
4. McEwen, B. S. & Sapolsky, R. M. (1995) *Curr. Opin. Neurobiol.* **5**, 205–216.
5. Sapolsky, R. M. (2000) *Neurobiol. Dis.* **7**, 540–542.
6. Bierhaus, A., Wolf, J., Andrassy, M., Rohleder, N., Humpert, P. M., Petrov, D., Ferstl, R., von Eynatten, M., Wendt, T., Rudofsky, G., *et al.* (2003) *Proc. Natl. Acad. Sci. USA* **100**, 1920–1925.
7. Epel, E. S., Blackburn, E. H., Lin, J., Dhabhar, F. S., Adler, N. E., Morrow, J. D. & Cawthon, R. M. (2004) *Proc. Natl. Acad. Sci. USA* **101**, 17312–17315.
8. Charney, D. S. (2004) *Am. J. Psychiatry* **161**, 195–216.
9. Carrasco, G. A. & Van de Kar, L. D. (2003) *Eur. J. Pharmacol.* **463**, 235–272.
10. McEwen, B. S. (2002) *The End of Stress as We Know It* (National Academies, Washington, DC), pp. 17–54.
11. Davidson, R. J. & Irwin, W. (1999) *Trends Cogn. Sci.* **3**, 11–21.
12. Dolan, R. J. (2002) *Science* **298**, 1191–1194.
13. Davidson, R. J. (2003) *Ann. N.Y. Acad. Sci.* **1000**, 316–336.
14. Sarter, M., Givens, B. & Bruno, J. P. (2001) *Brain Res. Rev.* **35**, 146–160.
15. Rosenkranz, M. A., Jackson, D. C., Dalton, K. M., Dolski, I., Ryff, C. D., Singer, B. H., Muller, D., Kalin, N. H. & Davidson, R. J. (2003) *Proc. Natl. Acad. Sci. USA* **100**, 11148–11152.
16. Davidson, R. J., Jackson, D. C. & Kalin, N. H. (2000) *Psychol. Bull.* **126**, 890–909.
17. Nutt, D. J. & Malizia, A. L. (2004) *J. Clin. Psychiatry* **65**, 11–17.
18. Detre, J. A. & Alsop, D. C. (1999) in *Functional MRI*, eds. Moonen, C. T. W. & Bandettini, P. A. (Springer, Heidelberg), pp. 47–62.
19. Aguirre, G. K., Detre, J. A., Zarahn, E. & Alsop, D. C. (2002) *NeuroImage* **15**, 488–500.
20. Wang, J., Aguirre, G. K., Kimberg, D. Y., Roc, A. C., Li, L. & Detre, J. A. (2003) *Magn. Reson. Med.* **49**, 796–802.
21. Wang, J., Li, L., Roc, A. C., Alsop, D. C., Tang, K., Butler, N., Schnall, M. D. & Detre, J. A. (2004) *Magn. Reson. Imaging* **22**, 1–7.
22. Wong, E. C. (1999) in *Functional MRI*, eds. Moonen, C. T. W. & Bandettini, P. A. (Springer, Heidelberg), pp. 63–69.
23. Kirschbaum, C., Pirke, K. M. & Hellhammer, D. H. (1993) *Neuropsychobiology* **28**, 76–81.
24. Soufer, R., Bremner, J. D., Arrighi, J. A., Cohen, I., Zaret, B. L., Burg, M. M. & Goldman-Rakic, P. (1998) *Proc. Natl. Acad. Sci. USA* **95**, 6454–6459.
25. Wang, J., Zhang, Y., Wolf, R. L., Roc, A. C., Alsop, D. C. & Detre, J. A. (2005) *Radiology* **235**, 218–228.
26. Furlan, P. M., DeMartinis, N., Schweizer, E., Rickels, K. & Lucki, I. (2001) *Biol. Psychiatry* **50**, 254–259.
27. Wang, J., Aguirre, G. K., Kimberg, D. Y. & Detre, J. A. (2003) *NeuroImage* **19**, 1449–1462.
28. Coan, J. A. & Allen, J. J. (2004) *Biol. Psychol.* **67**, 7–50.
29. Pascual-Leone, A., Catala, M. D. & Pascual-Leone Pascual, A. (1996) *Neurology* **46**, 499–502.
30. Phillips, M. L., Young, A. W., Scott, S. K., Calder, A. J., Andrew, C., Giampietro, V., Williams, S. C., Bullmore, E. T., Brammer, M. & Gray, J. A. (1998) *Proc. R. Soc. London Ser. B* **265**, 1809–1817.
31. Calder, A. J., Keane, J., Manes, F., Antoun, N. & Young, A. W. (2000) *Nat. Neurosci.* **3**, 1077–1078.
32. Davis, K. D., Taylor, S. J., Crawley, A. P., Wood, M. L. & Mikulis, D. J. (1997) *J. Neurophysiol.* **77**, 3370–3380.
33. Lange, C., Kracht, L., Herholz, K., Sachsse, U. & Irle, E. (2005) *Psychiatry Res.* **139**, 115–126.
34. Bonne, O., Gilboa, A., Louzoun, Y., Brandes, D., Yona, I., Lester, H., Barkai, G., Freedman, N., Chisin, R. & Shalev, A. Y. (2003) *Biol. Psychiatry* **54**, 1077–1086.
35. Nobili, F., Brugnolo, A., Calvini, P., Copello, F., De Leo, C., Girtler, N., Morbelli, S., Piccardo, A., Vitali, P. & Rodriguez, G. (2005) *Clin. Neurophysiol.* **116**, 364–375.
36. Sapolsky, R. M., Romero, L. M. & Munck, A. U. (2000) *Endocr. Rev.* **21**, 55–89.
37. Davidson, R. J. (1994) *Dev. Psychopathol.* **6**, 741–758.
38. Phan, K. L., Wager, T., Taylor, S. F. & Liberzon, I. (2002) *NeuroImage* **16**, 331–348.
39. Menon, V., Rivera, S. M., White, C. D., Glover, G. H. & Reiss, A. L. (2000) *NeuroImage* **12**, 357–365.
40. Frith, C. D. & Frith, U. (1999) *Science* **286**, 1692–1695.
41. Sinha, R., Lacadie, C., Skudlarski, P. & Wexler, B. E. (2004) *Ann. N.Y. Acad. Sci.* **1032**, 254–257.
42. Keay, K. A. & Bandler, R. (2001) *Neurosci. Biobehav. Rev.* **25**, 669–678.
43. Lupien, S. J. & McEwen, B. S. (1997) *Brain Res. Rev.* **24**, 1–27.
44. Vyas, A., Mitra, R., Shankaranarayana Rao, B. S. & Chattarji, S. (2002) *J. Neurosci.* **22**, 6810–6818.
45. Magarinos, A. M., McEwen, B. S., Flugge, G. & Fuchs, E. (1996) *J. Neurosci.* **16**, 3534–3540.
46. Gould, E., McEwen, B. S., Tanapat, P., Galea, L. A. M. & Fuchs, E. (1997) *J. Neurosci.* **17**, 2492–2498.
47. Drevets, W. C., Price, J. L., Simpson, J. R., Jr., Todd, R. D., Reich, T., Vannier, M. & Raichle, M. E. (1997) *Nature* **386**, 824–827.
48. Kirschbaum, C., Prussner, J. C., Stone, A. A., Federenko, I., Gaab, J., Lintz, D., Schommer, N. & Hellhammer, D. H. (1995) *Psychosom. Med.* **57**, 468–474.
49. McEwen, B. S. (2000) *Brain Res.* **886**, 172–189.

**NEUROSCIENCE**